Measurement of Neutron-Proton Polarization at 126 MeV*

A. S. CARROLL,† P. M. PATEL,‡ N. STRAX, AND D. MILLER
Cyclotron Laboratory, Harvard University, Cambridge, Massachusetts
(Received 8 March 1963)

The n-p polarization at 126 MeV has been measured between 33 and 82° c.m. by scattering a 41% polarized neutron beam from liquid hydrogen. The energy threshold and angle of scattering were determined by a range-threshold neutron counter. By the use of a conjugate counter to detect the recoil protons in coincidence with the scattered neutrons, the background rate was held to about 10%. Many systematic errors were eliminated by the use of precession magnets to reverse the sign of the neutron polarization. The maximum polarization was found to be 0.580 ± 0.040 at 56° c.m. This maximum is higher than that obtained in any of the Yale phase-shift predictions.

INTRODUCTION

THIS experiment is part of a program of free neutron-proton scattering experiments at the Harvard synchrocyclotron. Our objective is to perform a sufficient number of experiments so that with the use of charge independence the $T=0$ interaction can be uniquely determined at 126 MeV. The first experiment in this program was the measurement of the polarization and differential cross section for angles greater than 80° c.m. by Hobbie and Miller[1] where detection of the recoil proton with a range telescope is possible. Next, a measurement of the triple scattering parameter, D_t, was completed.[2] A measurement of the triple scattering parameter A_t' is in progress. In this experiment the neutron-proton polarization was determined in the angular range from 33 to 82° c.m., where the more difficult detection of the scattered neutron is necessary.

Neutron-proton polarization has been measured at other energies by scattering polarized neutrons from protons.[3–9] In some instances, this parameter has been extracted from inelastic scattering of polarized protons from deuterium.[10–12] The former method was chosen for this experiment since no corrections are needed for the presence of the third body as in p-D scattering.

POLARIZED NEUTRON BEAM

The beam depicted in Fig. 1 was that described by Miller and Hobbie[13] except for the addition of the precession magnets. The pole pieces and lead shielding inside the magnets collimated the beam to 2 in.×5 in. Additional shielding was placed near the neutron counter. The beam polarization as remeasured with the new configuration was 0.410 ± 0.017. The threshold on the neutron counter was set so that the distribution of neutrons detected had a roughly triangular spectrum as shown in Fig. 2. The mean energy at interaction was 126 ± 2 MeV.

The two precession magnets, extending along the length of the polarized neutron beam, enabled us to reverse the sign of the neutron polarization incident on the hydrogen target. Since identical scattering geometries were used for both signs of the incident polarization, systematic errors due to misalignments were eliminated. The correct magnetic field setting was calculated[14] to give a mean precession angle of 180°. This angle was checked experimentally. Including the effects of the beam energy spread, we calculated the component of the beam polarization normal to the scattering plane with the magnet on to be 0.986 ± 0.010 of that with the magnet off.

APPARATUS AND PROCEDURES

The angle and energy threshold of the scattered neutrons were defined by a 3-×6-×18-in. neutron counter, whose face was located 24 in. from the target center. This counter consisted of 16 pieces of $\frac{1}{8}$-in.-Pilot Scintillator B alternating with 16 equal-sized blocks of polyethylene.[15] A neutron was detected whenever it was converted in one of the polyethylene blocks, and the proton had sufficient energy to be detected by any 4 scintillators in succession. The threshold on the neutron counter was varied by changing the thickness of the polyethylene, so that the mean energy at interaction remained constant with scattering angle. The neutron counter efficiency as a function of energy was calculated

* Supported by the joint program of the U. S. Navy Office of Naval Research and the U. S. Atomic Energy Commission.
† Present address: Rutheford High Energy Laboratory, Chilton, Didcot, Berkshire, England.
‡ Present address: Laboratory of Nuclear Science, MIT Cambridge, Massachusetts.
[1] R. K. Hobbie and D. Miller, Phys. Rev. **120**, 2201 (1960).
[2] P. M. Patel, A. Carroll, N. Strax, and D. Miller, Phys. Rev. Letters **8**, 491 (1962).
[3] C. Whitehead, S. Tornabene, and G. H. Stafford, Proc. Phys. Soc. (London) **75**, 345 (1960).
[4] G. H. Stafford, C. Whitehead, and P. Hillman, Nuovo Cimento **5**, 1589 (1957).
[5] G. H. Stafford and C. Whitehead, Proc. Phys. Soc. (London) **79**, 430 (1962).
[6] R. T. Siegel, A. J. Hartzler, and W. A. Love, Phys. Rev. **101**, 838 (1956).
[7] W. Beneson, R. L. Walter, and T. H. May, Phys. Rev. Letters **8**, 66 (1962).
[8] R. B. Perkins and J. E. Simmons, Bull. Am. Phys. Soc. **8**, 37 (1963).
[9] P. H. Bowen, G. C. Cox, G. B. Huxtable, A. Langsford, J. P. Scanlon, and J. J. Thresher, Phys. Rev. Letters **7**, 248 (1961).
[10] A. F. Kuckes and R. Wilson, Phys. Rev. **121**, 1226 (1961).
[11] J. H. Tinlot and R. E. Warner, Phys. Rev. **124**, 890 (1961).
[12] O. Chamberlain, E. Segre, R. Tripp, C. Wiegand, and T. Ypsilantis, Phys. Rev. **105**, 288 (1957).
[13] D. Miller and R. K. Hobbie, Phys. Rev. **118**, 1391 (1960).
[14] V. Bargmann, L. Michel, and V. L. Telegdi, Phys. Rev. Letters **2**, 435 (1959).
[15] D. Miller and R. K. Hobbie, Rev. Sci. Instr. **31**, 621 (1960).

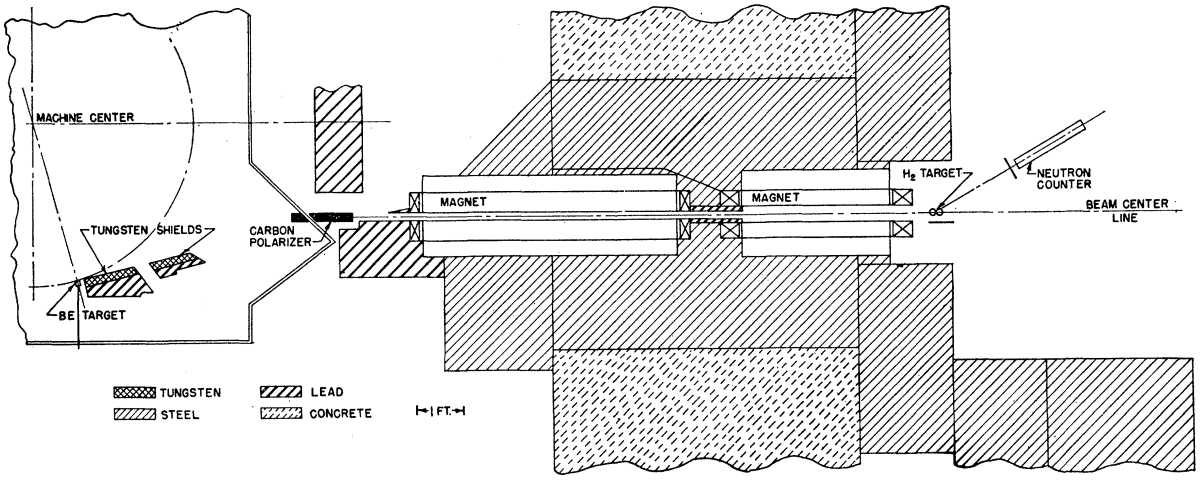

FIG. 1. Plan view of polarized neutron beam used in n-p polarization experiment.

using the range-energy curves,[16] n-p cross-section data,[17] and charge-exchange cross sections in carbon.[18,19] Since the energy threshold was based on a range requirement, and was insensitive to photomultiplier gain, the counter had the high degree of stability necessary for asymmetry measurements. The neutrons counter efficiency was about 1%. An $\frac{1}{8}$-in.-thick anti-coincidence counter which shielded the entire face of the neutron counter, eliminated counts due to protons from the target.

A preliminary survey of the background rate due to cosmic rays and due to neutrons which leaked through the shielding and which were scattered from the defining aperture of the collimator showed that the background rate was about 50 times the rate due to scattering from a 2-in.-diam liquid-hydrogen target. The separation of the production and polarization of neutrons, which produced a beam of high polarization,[13] unfortunately led to too low a ratio of beam intensity to background intensity for experiments in which the scattered neutron alone was detected. Since the background flux was too diffuse in direction to be adequately shielded, it became clear that it would be necessary to detect the low-energy recoil protons from the target in coincidence with the scattered neutrons in order to select only those neutrons which had been scattered from the target.

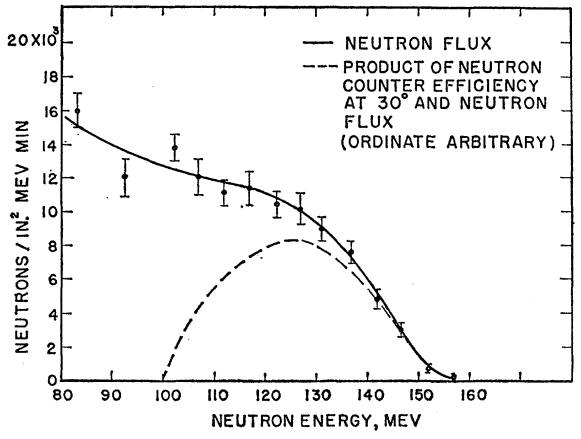

FIG. 2. Energy spectrum of polarized neutron beam. The dashed line shows the product of the neutron flux and the efficiency of the neutron counter at $\theta_{lab}=30°$.

The first technique tried utilized a block of Pilot Scintillator B ($C_{10}H_{11}$) as both a target and a detector of the recoil protons. However, a study of the coincidence pulse-height spectrum from the target scintillator indicated that the broad recoil proton peak contained about 30% more events than could be accounted for on the basis of n-p differential cross sections. These events were attributed to coincidences from carbon quasielastic (n,pn) and the decay products of inelastic carbon scattering $(n, n'\alpha$ and $n, n'\gamma)$. Since neither the cross section nor polarization for these events was accurately known, this method was not sufficiently accurate at this energy. With the intense, monoenergetic neutron beams available at about 20 MeV, the carbon contribution can be reduced to a few percent of the n-p scattering so that this method can be successfully employed.[7,8]

The counter geometry of the apparatus used in this experiment is shown in Fig. 3. With this apparatus, the recoil protons from two, 2-in.-diam cylinders of liquid hydrogen were detected by a $\frac{1}{16}$-in.-thick piece of scintillator located just outside the direct neutron beam. By placing the scintillator inside the vacuum chamber, protons emerging from the liquid hydrogen with energies as low as 3 MeV could be detected.

[16] M. Rich and R. Madey, University of California Radiation Laboratory Report No. UCRL-2301, 1954 (unpublished).
[17] W. H. Hess, Rev. Mod. Phys. **30**, 369 (1958).
[18] J. A. Hofmann and K. Strauch, Phys. Rev. **90**, 449 (1953); J. A. Hofmann, Ph.D. thesis, Harvard University, 1952 (unpublished).
[19] T. C. Randle, J. M. Cassels, T. G. Pickavance, and A. E. Taylor, Phil. Mag. **44**, 425 (1953).

Details of the construction of the liquid-hydrogen target and the recoil proton counter (conjugate counter) are shown in Fig. 4. Two cylinders of liquid hydrogen were used to create a relatively long narrow target. The cylinders were made of 0.003-in. Mylar and the outer Mylar windows were 0.010 in. The size of the scintillator (6 in.$\times 7\frac{1}{2}$ in. wide) was such that it defined the effective height of the hydrogen target and detected all the recoil protons which were associated with neutrons scattered into the neutron counter for all the angles studied.

By use of the recoil proton counter, the sources of background were limited to scattering from the Mylar cylinders and the recoil proton counter itself. This background rate varied from 6 to 18% of the rate from the liquid hydrogen. Random coincidences between the recoil-proton counter and neutron counter were always less than 7% of the true rate.

The principal problem associated with this method was that at laboratory scattering angles less than 30°, the recoil protons had insufficient energy to escape from the entire volume of liquid hydrogen. Since a coincidence was demanded with the recoil proton counter, only a crescent-shaped cylinder of hydrogen (such as that shown by the dotted line in Fig. 3) was effective. At 25° the effective volume was 85% of the entire volume, at 20° it was 42%, and at 16° it was 18%. Because of this effect, corrections to the scattering angle of about 0.6° and to the mean energy of about 3 MeV were necessary. The use of the precession magnets insured that no false asymmetries entered the measurements due to changes in the effective volume in right and left scatterings.

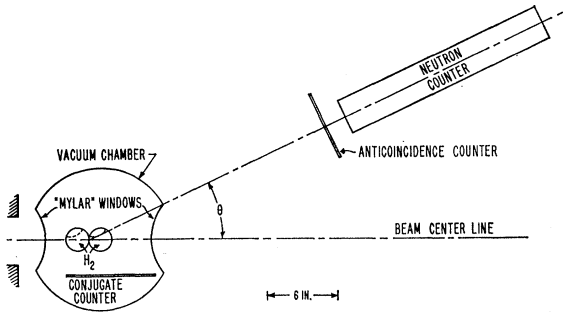

FIG. 3. The counter geometry for detection of neutrons scattered from liquid hydrogen.

A block diagram of the electronic circuits used in this experiment is shown in Fig. 5. Nearly all the circuits were built around a discriminator which used a tunnel diode to set the discrimination level, and a transistor operating in the avalanche mode to provide a fast trigger pulse.

The beam intensity was monitored by a BF_3 proportional counter which detected neutrons from the beryllium target. This monitor was unaffected by the presence of hydrogen in the target or the operation of the precession magnets.

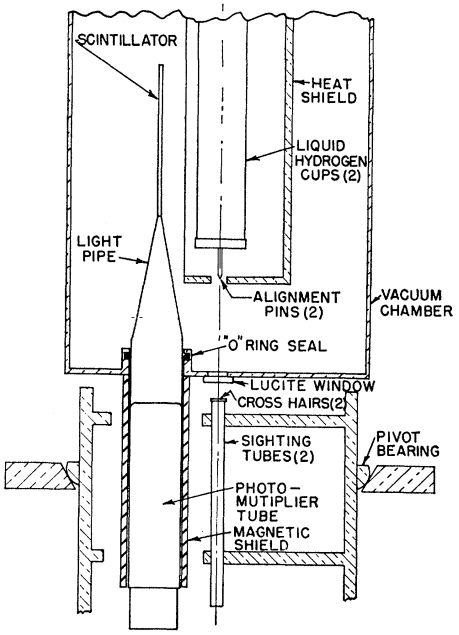

FIG. 4. Cross section of liquid-hydrogen target and pivot, showing details of construction of target and recoil proton counter. Also the target alignment procedure is illustrated.

The target and counter were aligned with respect to the axis of the beam pipe to $\pm\frac{1}{64}$ in. in the horizontal plane and to $\pm\frac{1}{16}$ in. in the vertical plane by means of a transit and the sighting tubes shown in Fig. 4. Final alignment of the neutron counter was achieved by moving the counter through the beam in 1° steps with

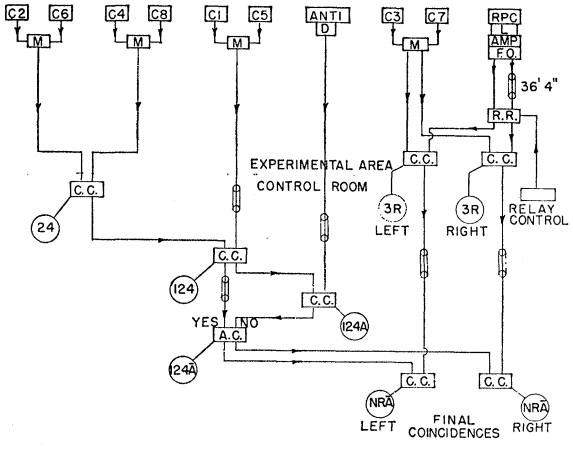

FIG. 5. Block diagram of electronic circuits. C1–C8 are the neutron counter photomultipliers which are coupled in pairs by the mixer circuits (M) (see Ref. 15 for details of neutron counter logic). (Left) and (Right) are interchangeable coincidence channels for measuring random coincidences. (RPC) recoil proton counter. (D) discriminator. (R.R.) reversing relay. (L) limiter. (C.C.) coincidence circuit. (A.C.) anticoincidence circuit.

the neutron precession angle set at $\pi/2$ to eliminate any polarization effects.

The effect of the field of the precession magnet on the photomultipliers was checked and found to be completely negligible.

DATA REDUCTION AND CORRECTIONS

The measured asymmetry, e_m, due to scattering from the liquid hydrogen was obtained from the final-coincidence rates with the magnet on and off:

$$e_m=[R_{\mathrm{H}}(\mathrm{on})-R_{\mathrm{H}}(\mathrm{off})][R_{\mathrm{H}}(\mathrm{on})+R_{\mathrm{H}}(\mathrm{off})]^{-1}, \quad (1)$$

where

$$R_{\mathrm{H}}(\mathrm{on})=[R_p{}^f(\mathrm{on})-R_d{}^f(\mathrm{on})]-[R_p{}^e(\mathrm{on})-R_d{}^e(\mathrm{on})] \quad (2)$$

and similarly for $R_{\mathrm{H}}(\mathrm{off})$. The superscripts in Eq. (2) refer to whether the target was full or empty, and the subscripts designate whether prompt or delayed coincidences were measured.

The effect of the background subtraction can be seen by expressing the measured asymmetry in an equivalent expression

$$e_m=e^f+r(1-r)^{-1}(e^f-e^e), \quad (3)$$

where

$$r=\frac{R_p{}^e(\mathrm{on})-R_d{}^e(\mathrm{on})+R_p{}^e(\mathrm{off})-R_d{}^e(\mathrm{off})}{R_p{}^f(\mathrm{on})-R_d{}^f(\mathrm{on})+R_p{}^f(\mathrm{off})-R_d{}^f(\mathrm{off})}. \quad (4)$$

e^f and e^e are the asymmetries measured with the target full and empty. The two terms in Eq. (3) are listed in Table I. About two-thirds of the background rate is due to scattering from the Mylar target cylinders, and the other third is from the recoil proton counter. Since for angles less than 30° the protons from the opposite side of the Mylar target cylinders cannot reach the recoil proton counter, an error equal to one-third the background correction term in Eq. (3) is applied to the data.

The mean energy of the neutrons at interaction as a function of the laboratory scattering angle and the polyethylene thickness in the neutron counter, $\bar{E}(\theta,t)$, is given by Eq. (5)

$$\bar{E}(\theta,t)=\int En(E)\sigma(\theta,E)V'(\theta,E)\epsilon(t,E_s)dE \Big/ \times\int n(E)\sigma(\theta,E)V'(\theta,E)\epsilon(t,E_s)dE. \quad (5)$$

The incident energy, E, is weighted by the product of four factors; the differential energy spectrum of the incident neutron beam $n(E)$, the differential cross section $\sigma(\theta,E)$,[17] the effective volume of the hydrogen target $V'(\theta,E)$, and the efficiency of the neutron counter $\epsilon(t,E_s)$ as a function of the polyethylene thickness, t, and the scattered neutron energy, E_s. E_s is related to E by the usual relativistic formula. The value of t was adjusted so that $\bar{E}(\theta,t)$ remained constant with angle. At angles less than 30° where the effective volume was less than 100% of the entire volume, the effective volume became larger with increasing energy. Since the high-energy neutrons were weighted more heavily, it was necessary to lower the neutron counter threshold to keep the mean energy at interaction constant. The threshold varied from 88.5 MeV at 16° to 99.5 MeV at the angles greater than 25°.

To check our understanding of the neutron counter efficiency and the effective volume calculations, we calculated the relative rates expected from known n-p differential cross sections and compared them with the experimentally observed rates. The results are shown in Table II. The errors on the calculated rates include the uncertainties in the differential cross section and the neutron counter threshold. The good agreement at all angles increases our confidence in the calculations.

The measured asymmetry at each angle is given by Eq. (5) if the asymmetry as a function of energy, $e(\theta,E)=P_b(E)P_{np}(\theta,E)$, is substituted for the incident energy E. The correction for the energy spread is the difference between the value of the asymmetry at 126 MeV and the integral over the entire energy interval. The integrals were evaluated using curves fitted to all the known n-p polarization data between 20 and 217 MeV[3–11] and to the nucleon-carbon polariza-

TABLE I. Measured asymmetries and corrections to be added to the measured asymmetries to give the corrected asymmetries.

Laboratory scattering angle	16	20	25	30	35	40
Target full asymmetry, e^f	0.145±0.017	0.178±0.010	0.220±0.010	0.220±0.014	0.167±0.015	0.117±0.015
Background correction $[r/(1-r)](e^f-e^e)$	0.031±0.017	0.007±0.006	0.009±0.005	0.012±0.006	0.016±0.007	−0.001±0.009
Measured asymmetry, e_m	0.176±0.024	0.186±0.012	0.228±0.013	0.232±0.016	0.184±0.017	0.116±0.020
Uncertainty in background subtraction	0.000±0.010	0.000±0.006	0.000±0.005	0.000±0.000	0.000±0.000	0.000±0.000
Energy spread	−0.002±0.001	−0.001±0.001	0.000±0.001	+0.001±0.001	+0.002±0.001	+0.003±0.001
Uncertainty in mean energy	0.000±0.007	0.000±0.008	0.000±0.009	0.000±0.008	0.000±0.006	0.000±0.003
Angular resolution	+0.001±0.001	+0.001±0.001	+0.001±0.001	+0.002±0.001	+0.002±0.001	+0.003±0.002
Uncertainty in mean scattering angle	0.000±0.002	0.000±0.001	0.000±0.001	0.000±0.001	0.000±0.001	0.000±0.002
Height of counter and target	0.000±0.002	+0.001±0.002	+0.002±0.002	+0.004±0.002	+0.004±0.002	+0.005±0.002
Anticoincidence counter efficiency	+0.003±0.004	+0.003±0.003	+0.002±0.002	0.001±0.001	0.000±0.001	0.000±0.001
Neutron precession angle	+0.001±0.001	+0.001±0.001	+0.001±0.001	+0.001±0.001	+0.001±0.001	+0.001±0.001
Total correction	+0.003±0.013	+0.005±0.011	+0.006±0.011	+0.009±0.009	+0.009±0.007	+0.012±0.005
Corrected asymmetry	0.179±0.027	0.191±0.016	0.234±0.017	0.241±0.018	0.193±0.018	0.128±0.021

tion between 95 and 200 MeV.[20] Then the results of the integration were compared to the values of the asymmetry given by the fitted curves at 126 MeV to give the correction. These same curves were used to estimate the error in the asymmetry due to the uncertainty in the mean energy of ±2 MeV.

The mean scattering angles were calculated by integrations over the hydrogen target volume and neutron counter width. These calculations took into account the following variations with angle; the neutron counter efficiency, the effective volume, and the differential cross section. The mean scattering angles differed by less than 1° from the nominal angles defined by the centers of the target and the neutron counter, except at 16° where the difference was 1.8°. Similar calculations were used to find the rms angular spread for the correction for the angular resolution. The rms spread was about 1.7° at all angles. Errors due to an uncertainty in the mean scattering angle of ±0.2° at 16° and of ±0.1° at all the other angles have been included.

TABLE II. Measured and calculated counting rates. 64 000 BF_3 monitor counts corresponds to about 27 min in time.

Laboratory scattering angle	Measured rates/ 64 000 BF_3	Calculated rates (normalized)/ 64 000 BF_3
16°	24.1±0.6	24.4±2.3
20°	46.7±0.6	43.9±3.3
25°	58.0±0.7	56.7±4.9
30°	42.8±0.7	43.3±4.0
35°	30.5±0.5	30.3±3.4
40°	19.0±0.3	20.7±1.9

Corrections were necessary for the finite height of the neutron counter and target since the scattering angle is slightly increased, and the asymmetry is reduced to $P_b P_{np} \cos\phi$, when the scattering plane deviates by an angle ϕ from the horizontal. As mentioned earlier, the normal component of the beam polarization with the magnet on was 0.986±0.010 of that with the magnet off so that a small correction was needed.

The anticoincidence counter efficiency was found to be 99±1%. A correction for this is included in Table I. The efficiency was raised to greater than 99.8%, and the asymmetry remeasured at 20° was found to be good agreement with the previous value.

The values of the *n-p* polarization were obtained by dividing the corrected asymmetries by the beam polarization measured in a carbon double-scattering experiment.

RESULTS AND DISCUSSION

Table III lists the six values of the *n-p* polarization at 126 MeV. The errors shown do not include the uncertainty in the beam polarization of ±0.017 which results in a maximum error of ±0.024 at 60° c.m. in the *n-p* polarization.

TABLE III. Neutron-proton polarization at 126 MeV. Error of ±4% in beam polarization has not been included. P_b=0.410 ±0.017.

Laboratory scattering angle	Center-of-mass scattering angle	Corrected asymmetry	Neutron-proton polarization
16°	33.0°	0.179±0.027	0.436±0.066
20°	41.2°	0.191±0.016	0.466±0.039
25°	51.5°	0.234±0.017	0.571±0.041
30°	61.7°	0.241±0.018	0.588±0.044
35°	71.8°	0.193±0.018	0.471±0.044
40°	81.9°	0.128±0.021	0.312±0.051

The polarization measured in this experiment at 126 MeV is displayed in Fig. 6 along with the larger angle data of Hobbie and Miller at 128 MeV.[1] Since the maximum change in the polarization in going from 126 to 128 MeV is 0.006, the experiments at 126 and 128 MeV can be directly compared. As seen from Fig. 6, the forward-angle data in this experiment join smoothly with the backward-angle data of Hobbie and Miller.

The values of the *n-p* polarization measured at 126 and 128 MeV are compared to the free *n-p* polarization measurements of Stafford and Whitehead at[4] 95 and[5] 140 MeV in Fig. 6, and to the Yale phase-parameter predictions at 128 MeV (based on an energy-dependent fit to earlier *n-p* measurements) in Fig. 7.[21] The four experimental points between 41.2 and 71.8° c.m. define the peak in the 126 MeV polarization curve quite accurately. An average of the values of the polarization at 51.5 and 61.7° c.m. give a peak polarization of 0.580±0.040 (error in the beam polarization included). This confirms the high peak suggested by the isolated points at 60° in the 95 and 140 MeV experiments.

The polarization data at 126 MeV indicate a higher peak polarization than any of the Yale phase-parameter

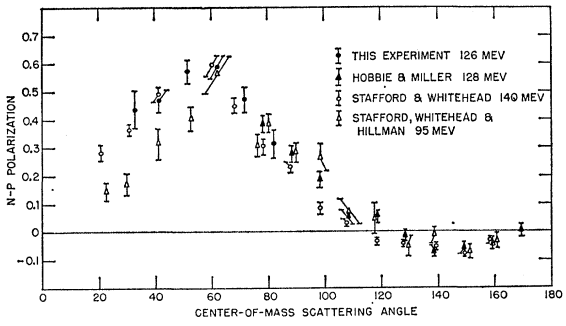

FIG. 6. Polarization in free neutron-proton scattering. The graph shows the present work and the larger angle data of Hobbie and Miller (Ref. 1). Also shown are the measurements Stafford and Whitehead made at 95 MeV (Ref. 4) and 140 MeV (Ref. 5).

[20] R. S. Harding, Phys. Rev. **111**, 1164 (1958); J. M. Dickson and D. C. Salter, Nuovo Cimento **6**, 239 (1957); R. Alphonce, A. Johansson, and G. Tibell, Nucl. Phys. **3**, 185 (1957); E. M. Hafner, Phys. Rev. **111**, 297 (1958).

[21] M. H. Hull, K. E. Lassila, H. M. Ruppel, F. A. McDonald, and G. Breit, Phys. Rev. **122**, 1606 (1961). We are indebted to the Yale group for computing and sending us the predictions at 128 MeV.

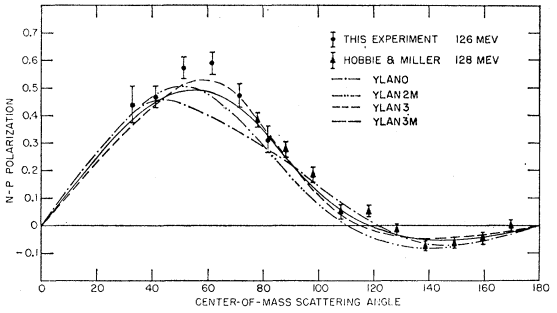

FIG. 7. The n-p polarization at 126 and 128 MeV (Ref. 1) in comparison to the Yale phase-shift predictions (Ref. 23). Not shown are solutions YLAN1 which follows the YLAN3M prediction and YLAN2 which is very similar to the prediction given by YLAN2M.

predictions, and seem to rule out the earlier solutions, YLAN0, YLAN2, and YLAN2M, at this energy. Of the remaining solutions, the polarization data at 126 MeV favor YLAN3 because of the higher peak in this prediction. In view of the discrepancies between the phase-parameter predictions and the earlier measurements,[21] however, these differences between the experimental points and the Yale phase-parameter curves should not be overemphasized. But it is interesting to note that the presently favored YLAN3M solution in this energy range was fitted to the p-n polarization derived from the inelastic p-d scattering experiment of Kuckes and Wilson at 143 MeV.[10] Theoretical corrections by Cromer and Thorndike[22] indicated that their peak polarization of 0.495 ± 0.017 should be raised by 0.03 ± 0.01 bringing it into closer agreement with the present experiment.

The measurement of the triple scattering parameter, D_t, at 128 MeV selects solution YLAN3M in preference to the other solutions, and since the YLAN3M solution, unlike the YLAN3 solution, can be joined smoothly to the quadrupole moment of the deuteron, we feel that the YLAN3M solution is an accurate representation of the data. However, modifications of the YLAN3M solution would result in better agreement with the double and triple scattering data at 126 MeV. With the differential cross section, polarization, and triple scattering data at this energy, the $T=0$ interaction should be well determined.

ACKNOWLEDGMENTS

We are grateful to the entire staff of the cyclotron laboratory for their assistance in making this experiment possible. The help of many research assistants in assembling apparatus and collecting data is gratefully acknowledged. One of us (A.S.C.) is grateful for the support of a National Science Foundation Graduate Fellowship for the years 1958 to 1962.

[22] A. Cromer and E. Thorndike (to be published).

PHYSICAL REVIEW VOLUME 134, NUMBER 3B 11 MAY 1964

Tests of the One-Pion-Exchange Model

ALFRED S. GOLDHABER*
Palmer Physical Laboratory, Princeton, New Jersey
(Received 24 December 1963)

The original Chew-Low proposal of a pion pole in the collision matrix at unphysical momentum transfer has evolved into a "generalized Born approximation" for one-pion exchange (OPE). This predicts that the collision amplitude will be independent of the total center-of-mass energy W for the reaction. The author describes tests of this prediction for the process $\pi+N\rightarrow N+2\pi$, where the final dipion mass is in the vicinity of the ρ resonance at 750 MeV, using data for incoming pion momenta of 1.4, 1.7, and 3.0 BeV/c. The results agree with the model except for a variation with W of the angular distribution of the dipion decay with respect to the incident π direction.

I. INTRODUCTION

IN recent years people have often tried to describe collisions of elementary particles by a "generalized Born approximation," that is, by writing a lowest order perturbation theory matrix element, in which the coupling constants at each vertex are replaced by "form factors," arbitrary functions of the invariants which may be formed from the four-momenta meeting at the vertex. As a rule, only one of the possible lowest order matrix elements is used because experimental precision is not yet great enough to justify a more elaborate analysis with superposition of several different terms in the collision amplitude. Thus, the method is only useful when one term seems to dominate the amplitude. I shall outline the development of one such model, the one-pion-exchange (OPE) model, for the process,

$$\pi^-+p\rightarrow\begin{cases}\pi^-+\pi^++n & \text{(1a)}\\ \pi^-+\pi^0+p, & \text{(1b)}\end{cases}$$

and describe some tests of the model. The tests are

* National Science Foundation Predoctoral Fellow.